Planta (1989) 178:164–175

Planta

Gas-exchange of ears of cereals in response to carbon dioxide and light

II. Occurrence of a $C_3 - C_4$ intermediate type of photosynthesis

Alexander Ziegler-Jöns
Lehrstuhl für Physik Weihenstephan, Technische Universität München, D-8050 Freising 12, Federal Republic of Germany

Abstract. Data for the maximum carboxylation velocity of ribulose-1,5-biosphosphate carboxylase, V_m, and the maximum rate of whole-chain electron transport, J_m, were calculated according to a photosynthesis model from the CO_2 response and the light response of CO_2 uptake measured on ears of wheat (*Triticum aestivum* L. cv. Arkas), oat (*Avena sativa* L. cv. Lorenz), and barley (*Hordeum vulgare* L. cv. Aramir). The ratio J_m/V_m is lower in glumes of oat and awns of barley than it is in the bracts of wheat and in the lemmas and paleae of oat and barley. Light-microscopy studies revealed, in glumes and lemmas of wheat and in the lemmas of oat and barley, a second type of photosynthesizing cell which, in analogy to the Kranz anatomy of C_4 plants, can be designated as a bundle-sheath cell. In wheat ears, the CO_2-compensation point (in the absence of dissimilative respiration) is between those that are typical for C_3 and C_4 plants.

A model of the CO_2 uptake in C_3–C_4 intermediate plants proposed by Peisker (1986, Plant Cell Environ. **9**, 627–635) is applied to recalculate the initial slopes of the $A(p^c)$ curves (net photosynthesis rate versus intercellular partial pressure of CO_2) under the assumptions that the J_m/V_m ratio for all organs investigated equals the value found in glumes of oat and awns of barley, and that ribulose-1,5-bisphosphate carboxylase is redistributed from mesophyll to bundle-sheath cells. The results closely match the measured values. As a consequence, all bracts of wheat ears and the inner bracts of oat and barley ears are likely to represent a $C_3 - C_4$ intermediate type, while glumes of oat and awns of barley represent the C_3 type.

Key words: *Avena* (photosynthesis) – C_3–C_4 intermediate photosynthesis – *Hordeum* (photosynthesis) – Inflorescence (cereal ear) – Photosynthesis – *Triticum* (photosynthesis)

Abbreviations: A = net photosynthesis rate ($\mu mol \cdot m^{-2} \cdot s^{-1}$); J_m = maximum rate of whole-chain electron transport ($\mu mol \cdot e^- \cdot m^{-2} \cdot s^{-1}$); p^c (μbar) = intercellular partial pressure of CO_2; PEP = phosphoenolpyruvate; PPFD = photosynthetic photon flux density (μmol quanta $\cdot m^{-2} \cdot s^{-1}$); RuBPCase = ribulose bisphosphate carboxylase/oxygenase; RuBP = ribulose bisphosphate; V_m = maximum carboxylation velocity of RuBPCase ($\mu mol \cdot m^{-2} \cdot s^{-1}$); $\Gamma^* = CO_2$ compensation point in the absence of dissimilative respiration (μbar)

Introduction

Ears of wheat were found to differ markedly from leaves in the CO_2 response of photosynthetic CO_2 uptake and stomatal conductance (Knoppik et al. 1986). Besides the greater amount of dissimilative (i.e. non-photorespiratory) respiration in the dark and in the light caused by the respiration of the grains and the higher amount of heterotrophic tissue in the bracts, ears show higher maximum rates of CO_2 uptake (at high photosynthetic photon flux density (PPFD) and high CO_2) in relation to the CO_2 uptake at normal atmospheric CO_2. In the first part of this study (Ziegler-Jöns 1989), this characteristic was evident in all bracts of the wheat ears and in lemmas and paleae (here called "inner bracts") of oat and barley ears, but not in glumes of oat and awns of barley. Hence the characteristic differences between leaves and ears result from properties of the individual bracts and not from the special arrangement of these bracts in the ear.

In order to do study these properties, the CO_2-response curves of net photosynthesis at saturating PPFD as well as the light-response curves at saturating CO_2 were measured on intact ears and on ears from which either the glumes (oat, wheat) or the awns (barley) or the inner bracts (oat, wheat) had been removed. These curves were evaluated according to the photosynthesis model proposed

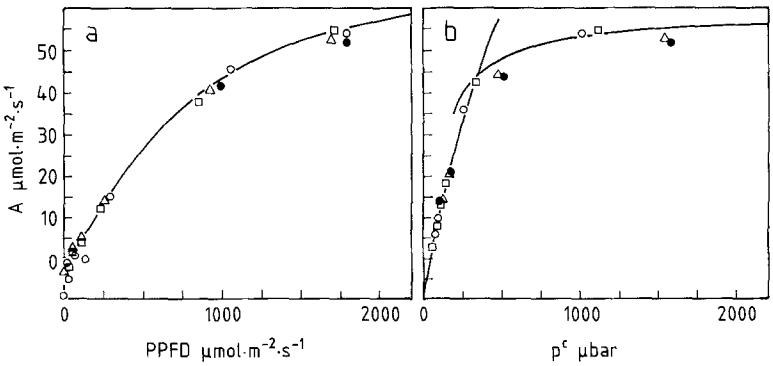

Fig. 1a, b. Net photosynthesis rates in response to PPFD at high CO_2 (**a**) and in response to CO_2 at high PPFD (**b**). All measured data of replications on four intact barley ears before anthesis are shown. The model curves (*solid lines*) represent the mean values of the parameters calculated from the individual ears according to the method described in *Appendix A*

by Farquhar et al. (1980) and Farquhar and von Caemmerer (1982). The mathematical methods for the fitting of the measured curves are described by Selinger et al. (1987), Ziegler-Jöns and Selinger (1987), and briefly in *appendix A*.

In addition, cross sections of the bracts were studied by light microscopy in order to reveal differences between the bracts in the structure of the mesophyll.

Material and methods

Plant material. Seeds of spring wheat (*Triticum aestivum* L. cv. Arkas), barley (*Hordeum vulgare* L. cv. Aramir) and oat (*Avena sativa* L. cv. Lorenz) were sown and grown exactly as described by Ziegler-Jöns (1989).

Treatments of plants. Wheat and oat were not treated, ear intact (*N*), the glumes removed (*I*) or the paleae, lemmas and grains removed (*II*). Additional treatment: glumes and grains removed. *Barley* was not treated, ear intact (*N*) or the awns removed (*III*). For an explanation of the terms (see Ziegler-Jöns 1989 and Radley 1981).

Treatments were carried out on the afternoon before gas-exchange measurements so that the wound respiration could ease off, but no adaptation, e.g. to changed light conditions could begin.

After the end of the gas-exchange measurements the reference area (i.e. half of the area of an enveloping prism for wheat ears; for oat and barley the projective area measured by use of an areameter) of the ears was determined.

In the spring of 1987 seeds of all three cultivars were sown as described above to carry out supplementary measurements. In order to determine the influence of the CO_2 and H_2O release of the grains on the gas-exchange characteristics, attempts were made to remove the grains from the lemmas after removal of the outer parts. This proved difficult with wheat and oat, but impossible for barley, where the grains stick fast to the lemmas.

Gas-exchange measurements. Gas-exchange measurements started at the end of June with the beginning of ear emergence. Gas exchange was measured in an open system as described in detail by Knoppik et al. (1986) and in a short summary by Ziegler-Jöns (1989). Gas-exchange rates were calculated according to von Caemmerer and Farquhar (1981).

The measurements comprised CO_2- and H_2O-exchange rates in response to CO_2 partial pressure at saturating PPFD (>1500 µmol·m^{-2}·s^{-1}) and in response to PPFD at saturating CO_2 (2000 µbar ambient).

All experiments were done in the same order and for the same period of time and were replicated on four to six ears of each treatment during the period before anthesis as well as two weeks after anthesis. However, as the time course plays a minor role for the topic of this study, only the data for the measurements before anthesis are shown.

The measured CO_2-response curves at high PPFD and light-response curves at high CO_2 were fitted on the basis of the model proposed by Farquhar and von Caemmerer (1982) according to Selinger et al. (1987) and Ziegler-Jöns and Selinger (1987). An outline of the mathematical methods of curve fitting and parameter calculation is given in *Appendix A*. Parameter calculation by curve fitting is done for each single measurement, and the resulting values for the parameters of each treatment averaged. Model curves for all replications of one treatment represent these mean values. Figure 1 gives an example for intact barley ears before anthesis. Obviously, the CO_2 response as well as the light response of CO_2 uptake are well represented by the numerical values for the model parameters. For the purpose of clarity, data are only given for the parameters V_m and J_m (Table 1).

The compensation points in the absence of dissimilative respiration, Γ^*, of two intact wheat ears and one of treatment *I* were measured according to Brooks and Farquhar (1985): at various (low) PPFDs, the $A(p^c)$ curves were measured at low p^c, and Γ^* calculated as the intersection of the individual $A(p^c)$ curves.

Appendix B gives equations for the calculation of the initial slope of the $A(p^c)$ curve from numerical values for the maximum carboxylation velocity, V_m, and the distribution of ribulose-1,5-bisphosphate carboxylase/oxygenase (RuBPCase) between mesophyll and bundle sheath cells according to a model proposed by Peisker (1986).

Light microscopy. Cross sections of glumes, lemmas and paleae of wheat and oat were examined microscopically in order to determine morphological differences. Three cross sections were prepared for each bract: one from the top, one from the middle part, and one from the lower part. In addition, one cross section was done for the oat awn. Immediately after removal from the ear the bracts were fixed. The fixatives (OsO_4, glutaraldehyde) were applied in 0.1 M Sörensen buffer (pH 7.4). The contrast was enhanced by adding salts of heavy metals. Complete dehydration of the tissue was effected with ethanol as a mediator medium. Ethanol was replaced by fluid polymers (epoxide polymers of low viscosity, e.g. Epon, ERL) to permeate the tissue completely. Polymerization was effected at 70° C. Semithin sections were cut on an ultramicrotome and examined under the lightmicroscope.

In addition, fresh cuts of awns of barley were examined under the light microscope.

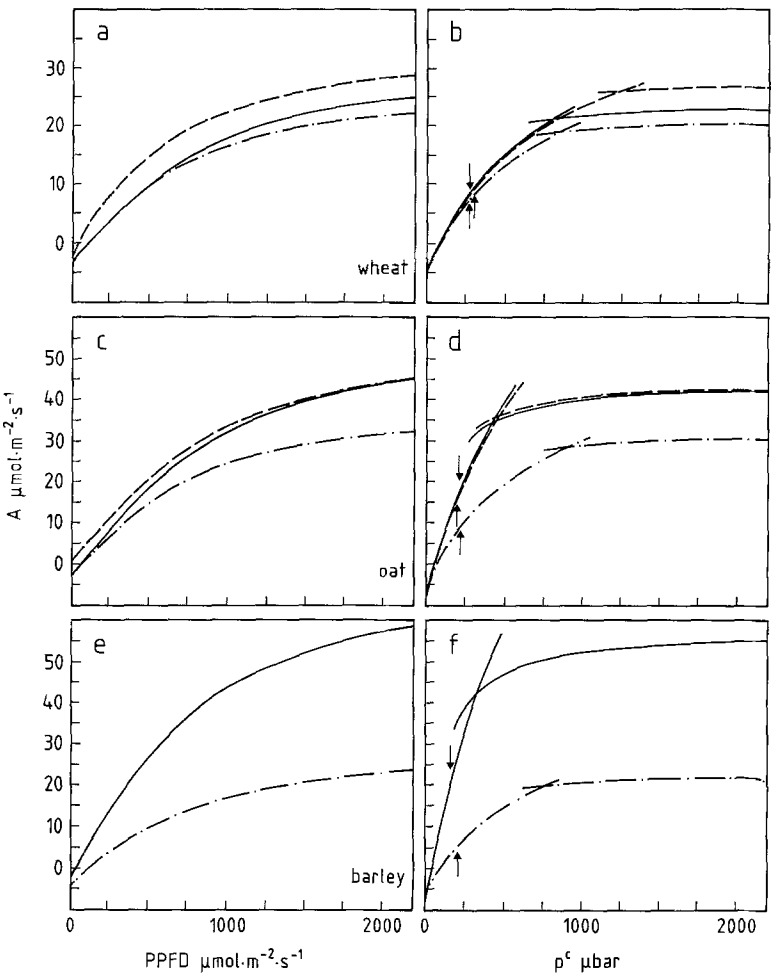

Fig. 2a–f. Model curves representing the means of the photosynthetic parameters calculated from four to six replications. **a, c, e**: light-response curves at high CO_2; **b, d, f**: CO_2-response curves at high PPFD; **a, b**: wheat; **c, d**: oat; **e, f**: barley. Intact ears (*solid lines*), inner bracts (*dotted lines*), glumes (*dashed lines*) are shown. *Arrows* indicate the intercellular partial pressures of CO_2 under normal atmospheric conditions

Results

Wheat. Figure 2a, b shows the modelled $A(I)$ (I = incident PPFD) and $A(p^c)$ curves for all treatments of wheat ears before anthesis. The broken lines represent the curves for the glumes (treatment *II*). The $A(I)$ curve lies above the others, since dissimilative respiration in the light is lower when grains are missing. The curves for the inner bracts (treatment *I*) coincide with those for the intact ears in the beginning, but drop later on. Differences between treatment *I* and *II* are less significant than in oat.

Intercellular CO_2 partial pressures at normal atmospheric CO_2 are indicated in the $A(p^c)$ curves by arrows. The three treatments *N*, *I*, *II* hardly differ in this regard. They differ slightly in the value of CO_2 partial pressure at which limitation of photosynthesis switches from carboxylation velocity to ribulose-1,5-bisphosphate (RuBP)-regeneration velocity (intersection of the two partial curves in Fig. 2b).

In the intact ear the inner bracts receive less light than the glumes so that the incident PPFD is not representative for the supply of light to all parts of the ear. Model calculations for the intact ears can therefore only be used to calculate the curves representing the mean of all replications and show the graph, and the resulting photosynthetic parameters have no physiological meaning. Hence, values of the parameters are not given for treatment *N* in Table 1.

The calculated maximum rate of whole-chain electron transport, J_m, and the maximum carboxylation velocity of RuBPCase, V_m, are lower in ears of treatment *I* (inner bracts) than in those of treatment *II* (glumes). The ratio J_m/V_m is similar in ears of the two treatments (as opposed to the results in oat and barley).

Figure 3 shows the result of a measurement of the CO_2-compensation point in the absence of dissimilative respiration, Γ^*, on intact wheat ears. Obviously, the intersection of all individual CO_2-response curves is near 18 µbar and hence below the values reported in the literature for Γ^* of C_3 plants. Replications of the measurement with ears

Table 1. Photosynthetic parameters calculated from fittings of the $A(p^c)$ curve at saturating PPFD and from the $A(I)$ (I = incident PPFD) curve at saturating CO_2. Values for inner (treatment *I*) and outer (*II*) bracts of wheat and oat and for intact (*N*) and awnless (*III*) ears of barley before anthesis. Rates refer to the half of the enveloping area (wheat) or the projective area (oat, barley), and are the means ±SE of four to six replications. J_m = maximum rate of whole-chain electron transport ($\mu mol\ e^- \cdot m^{-2} \cdot s^{-1}$); V_m = maximum carboxylation velocity of RuBPcase ($\mu mol \cdot m^{-2} \cdot s^{-1}$)

	J_m	V_m	J_m/V_m
Wheat			
I	152.9± 8.6	42.9±4.1	3.7±0.9
II	185.3±17.6	48.4±2.4	3.8±0.3
Oat			
I	204.7±21.7	59.2±2.8	3.4±0.2
II	264.3±20.1	112.0±5.4	2.3±0.2
Barley			
III	179.4± 9.6	49.2±3.3	3.7±0.3
N	358.5±14.4	164.9±5.8	2.2±0.1

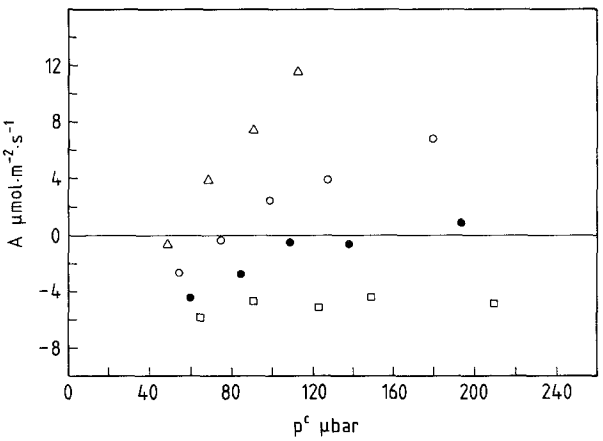

Fig. 3. Carbon dioxide response of net photosynthesis of intact wheat ears at various PPFDs (29 (□), 90 (+), 200 (◇), 600 (△) $\mu mol \cdot m^{-2} \cdot s^{-1}$) for the evaluation of the CO_2-compensation point in the absence of dissimilative respiration, Γ^*, according to Brooks and Farquhar (1985)

from which the glumes had been removed show the same result.

Oat. Figure 2c, d shows the modelled curves for all treatments before anthesis. The curves for intact ears (solid line) and for glumes (dashed line) are very similar, the initial part of the $A(I)$ curve of the former lying lower by the amount of dissimilative respiration in the grains. The $A(I)$ curve and the $A(p^c)$ curve for the inner bracts lie below the others. In contrast to wheat, the transition from saturating RuBP to limiting RuBP is substantially lower in the CO_2-response curves of the glumes. Intercellular CO_2 partial pressure under normal atmospheric conditions (as shown by arrows) is almost identical in the three treatments.

The curves for the intact ears coincide with those for treatment *II*, except in the initial part of the $A(I)$ curves. This is in contrast to the situation in wheat and caused by the fact that the reference areas of the treatments *N* and *II* do not differ markedly in the period before anthesis. The $A(I)$ curves for intact ears are a combination of the curves for the treatments *I* and *II* and, as described above for wheat, the mean values of the parameters of intact ears can be used only for the graphic representation. Only treatments *I* and *II* should be considered for physiological evaluations.

The maximum rates of whole-chain electron transport, J_m, (Table 1) are lower in the inner bracts than in the glumes. The same applies to the maximum velocity of carboxylation of RuBP-Case. In oat, inner bracts have higher values of J_m/V_m than glumes. Values for the latter can be compared to those for barley awns, values for the former can be compared to all bracts of wheat and inner bracts of barley.

Barley. Figure 2e, f shows the model curves of the two treatments before anthesis. The curves for treatment *III* (awnless ears) lie below those of the intact ear, and the differences are more pronounced than in the other species. The intersection of the two partial $A(p^c)$ curves and the CO_2 partial pressure under atmospheric conditions (arrows) for treatment *N* are the highest of all treatments of the three species.

In barley, as opposed to wheat and oat, components of the ear do not shade each other. Therefore the model calculation can be applied to the intact ear as well. The calculated maximum rate of whole-chain electron transport and the maximum velocity of carboxylation of intact ears are higher than those of awnless ears (Table 1). The awns are the most active organs in all treatments of all species, while the bracts of barley can be compared to those of other species.

In the intact ears (and therefore in the awns, which contribute approx. 90% to the gas exchange of the intact ear, Ziegler-Jöns 1989) the ratio J_m/V_m is comparable to that of glumes of oat.

Light microscopy. The results from the Γ^* measurements on wheat ears were the motive for looking for signs of a Kranz-anatomy in the individual bracts. The glumes of wheat ears show bundle-sheath cells surrounding the big vascular bundles and also the smaller vascular bundles (Fig. 4). The

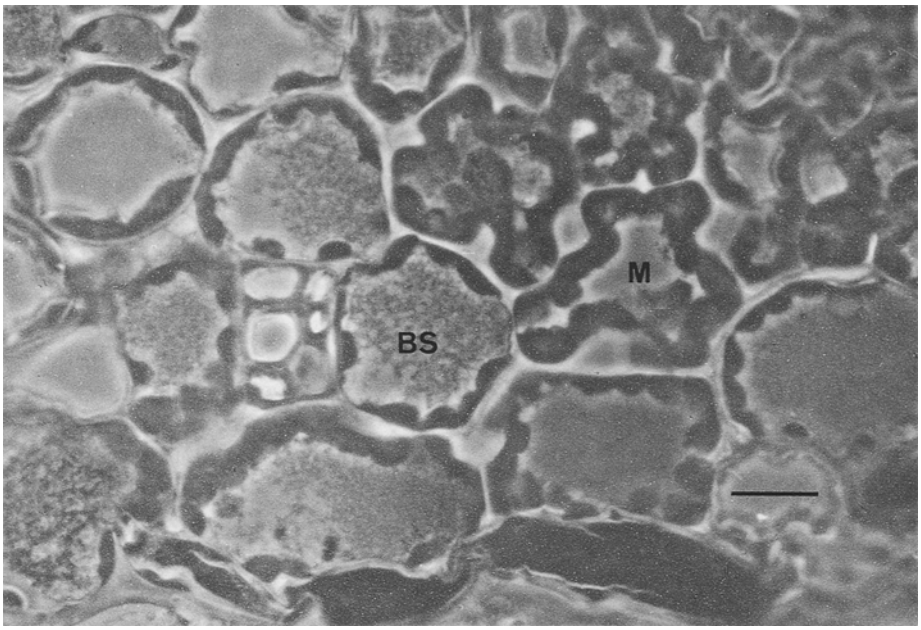

Fig. 4. Cross section of a glume of wheat. *BS*=bundle-sheath cell; *M*=normal mesophyll cell. Bar=10 μm

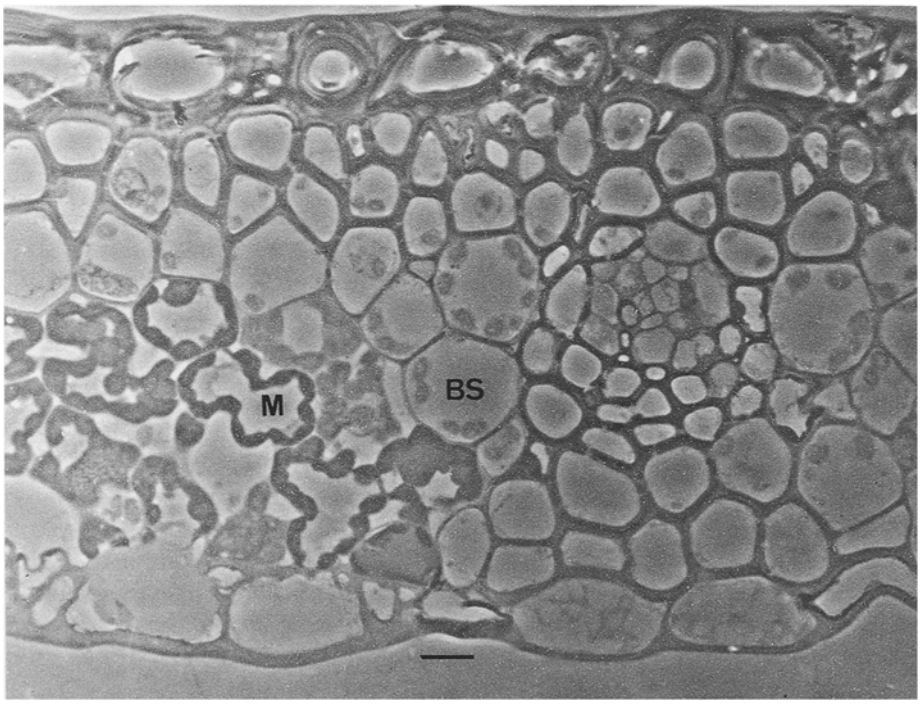

Fig. 5. Cross section of a lemma of wheat. *BS*=bundle-sheath cell; *M*=normal mesophyll cell. Bar=10 μm

latter occur in the spongy parenchyme and often consist only of two tracheids and one sieve-tube element. Bundle-sheath cells look less lobed than mesophyll cells; the cell walls appear to be thicker, and the chloroplasts appear less dark, with light flecks which could be interpreted as starch grains. In contrast to the Kranz anatomy in C_4 leaves, the chloroplasts in the bundle-sheath cells are evenly distributed and of the same size as in mesophyll cells. The same type of bundle-sheath cells can be found in the lemmas of wheat (Fig. 5) and of oat. Bundle-sheath cells are often found in the zone between spongy parenchyme and sclerenchyme, as well. They are, however, absent in the glumes of oat (Fig. 6) and in the awns of oat and barley (not shown).

Fig. 6. Cross section of a glume of oat. *M* = normal mesophyll cell. Bar = 10 µm

Discussion

The characteristic differences between ears and flag leaves of wheat reported by Knoppik et al. (1986) and Ziegler-Jöns et al. (1987) were also found in parts of the ears of oat and barley, but not in the glumes of oat or in the awns of barley (Ziegler-Jöns 1989). Both the latter showed ratios of the maximum CO_2 uptake to the CO_2 uptake at normal atmospheric CO_2 that were similar to those for leaves, while for all other parts of ears under examination this ratio was significantly higher.

In the data presented here, these characteristics are reflected by the ratio of maximum rate of whole-chain electron transport to maximum carboxylation velocity of RuBPCase, J_m/V_m. These data are the results of fittings of the light-response curves (J_m) and the $A(p^c)$ curves (V_m) and are independent of stomatal mechanisms or different CO_2 compensation points of the treatments. However, the calculation of V_m (compare *Appendix A*) requires the correct estimation of the intercellular CO_2 partial pressure. Thus, only if the calculation of p^c is not erroneous, the J_m/V_m ratio reveals differences between parts of the ears in the properties of the photosynthesizing tissue.

Intercellular partial pressure of CO_2. As can be seen from Fig. 2d, considerable errors would have to be made in the calculation of the intercellular partial pressure of CO_2 in order for the differences, e.g. between glumes and inner bracts of oat ears, to result. The correction of these errors should result in a shift of the calculated intercellular partial pressures of CO_2 for the inner bracts to the left by approx. 100 µbar at normal atmospheric CO_2. The possible sources of errors in the calculation of p^c are listed here.

(i) The intercellular air spaces of the bracts are not saturated with water vapor. However, the correction of this effect would cause a shift of the calculated intercellular partial pressure of CO_2 to the right, because, for a given rate of transpiration, the real conductivity to H_2O would have been underestimated.

(ii) The measurement of the temperature of the bracts contains errors, which are greater than 5 K. However, besides the fact that such great errors seem to be unreasonable, because the thermocouples were calibrated under measurement conditions (Ziegler-Jöns et al. 1986), these errors are equal for all treatments of the ears and cannot explain the differences.

(iii) There is an additional source of transpiration that is not related to CO_2 uptake. Possible sources are the grains or the cuticle. To produce the differences between inner and outer bracts, more than 70% of the transpiration of the inner bracts would have to come from the grains or the cuticles of the inner bracts, but not from the cuticle of the glumes. From typical conductivities of cuticles (Schönherr 1982; Laisk 1983; Meidner 1986) maximum contributions of the cuticles to the transpiration of treatment *I* (inner bracts) of oat can be estimated at 10%. On the other hand, the H_2O release of the grains cannot attain rates neccessary

to explain the characteristics (Jenner and Rathjen 1972; C.F. Jenner, Waite Institute, Adelaide, Australia, personal communication). In addition, in the 1987 experiments the grains were removed from ears of treatment *I* of wheat and of oat. The transpiration of the ears was not reduced in this treatment; on the contrary, transpiration was enhanced by the additional transpiration through the stomata that are blocked by the growing grains in intact ears (Ziegler-Jöns 1989). Hence, transpiration by the grains or through the cuticle cannot explain the differences between glumes and inner bracts of oat.

(iv) Additional CO_2 release by the grains and partial refixation in the bracts. This process would cause a parallel shift of the $A(p^c)$ curve without changing the slope and can therefore not explain the characteristics.

Moreover, the arrows in Fig. 2 indicate that the intercellular partial pressure of CO_2 at normal atmospheric CO_2 is nearly the same for inner and outer bracts. Therefore, the regulation of the intercellular CO_2 by the stomata in all bracts appears to work in the same way and to depend upon the photosynthetic capacity of the mesophyll (compare Wong et al. 1985a, b, c).

The characteristic differences between parts of the ears can therefore not be ascribed to errors in the calculation of the intercellular partial pressure of CO_2. It must be assumed that physiological differences are responsible for the characteristic J_m/V_m ratios.

Occurrence of a C_3–C_4 intermediate type of photosynthesis. C_3–C_4 intermediate plants have CO_2-compensation points that are between those of C_3 and C_4 plants (for review see Apel and Peisker 1979) and show a biphasic response to O_2 (Peisker and Bauwe 1984). The CO_2-compensation point is high in ears (> 50 µbar at 25° C, Knoppik et al. 1986) because of the high rates of dissimilative respiration in the light, so that it cannot prove the presence or absence of C_3–C_4 intermediate characteristic. Therefore, the method proposed by Brooks and Farquhar (1985) was used to measure the CO_2-compensation point without dissimilative respiration. For leaves of C_3 plants, typical values for Γ^* of 31 µbar (Farquhar and von Caemmerer 1982), 40 µbar (Brooks and Farquhar 1985) and 44 µbar (Harley et al. 1986) were reported at 25° C. The values for Γ^* are expected to be below 10 µbar for C_4 leaves and between 15 and 25 µbar for leaves of C_3–C_4 intermediate plants. In this study, Γ^* was found to be approx. 18 µbar (Fig. 3) in wheat ears and hence typical for the values reported for Γ^* of C_3–C_4 intermediate plants.

Among C_3–C_4 intermediate species, there are species that exhibit a true Kranz anatomy, but also intermediates between true Kranz (C_4) and non-Kranz (C_3) types (Holaday et al. 1984). The enzyme RuBPCase is found in both mesophyll cells and bundle-sheath cells (Perrot-Rechenmann et al. 1984), but appears to be redistributed in some species, so that the RuBPCase content is lower in mesophyll cells than in bundle-sheath cells (Peisker 1986).

The glumes of wheat ears show a second type of cell surrounding the big vascular bundles and also the smaller vascular bundles (Fig. 4). The cell walls of this type appear to be thicker and they contain evenly distributed chloroplasts. The same type of bundle-sheath cell can be found in the lemmas of wheat (Fig. 5) and of oat. These cells are, however, absent in the glumes of oat (Fig. 6) and in the awns of oat and barley. The bracts of wheat and the inner bracts of oat therefore represent intermediates between true Kranz and non-Kranz types.

To explain the intermediate values of the CO_2-compensation point of C_3–C_4 intermediate species, it has been suggested that the close association of chloroplasts and mitochondria in the bundle-sheath cells increases the refixation of photorespired CO_2 in these cells and thus lowers the apparent rate of photorespiration (Brown 1980). Hunt et al. (1987) claim that this cannot explain the low rates of apparent photorespiration (which are, however, underestimated by the methods used for the calculation, Gerbaud and André 1987), because effective recapture of CO_2 seems to be unlikely in mesophyll cells. Moreover, the hybrids between C_3 and C_3–C_4 species of *Panicum* can show the same CO_2-compensation point as the C_3 parent, though having the anatomical characteristics of the C_3–C_4 parent (Bouton et al. 1986).

Rawsthorne et al. (1988) suggest that the recapture of photorespired CO_2 is improved by a localisation of the decarboxylation of glycine in the bundle-sheath cells. They have found a very much lower capacity to decarboxylate glycine in the mesophyll cells than in the bundle-sheath cells of leaves of *Moricandia arvensis*; this situation is similar to that in C_4 plants.

Furthermore, it has been suggested that the intermediate features could be the consequence of a small amount of CO_2 fixation via the C_4 pathway (Rathnam and Chollet 1979). As in C_4 plants, Perrot-Rechenmann et al. (1984) found phosphoenolpyruvate carboxylase (PEPCase) exclusively in the cytosol of the mesophyll cells of *Panicum milioides*. The occurence of a C_4 cycle of limited capacity

seems probable in some *Flaveria* species (Bauwe 1984), and in leaves of cassava (Cock et al. 1987). On the other hand, Hunt et al. (1987) found no evidence for a C_4 cycle in *Moricandia arvensis*, and the activities of the enzymes characteristic of the C_4 cycle are no greater in leaves of this species than in those of C_3 species (Holaday et al. 1981).

Wirth et al. (1977) report higher activities of C_4 enzymes in parts of wheat and oat ears than in leaves. The bracts of the ears have RuBPcase contents which amount to approx. 20% and 25–30% of the values for the flag leaves of wheat and oat, respectively. However, the activities of PEPCase in the bracts are twice as high as in the flag leaves, being highest in the glumes. The higher PEPcase activities are also accompanied by higher amounts of C_4 products of CO_2 fixation: 10% (oat) to 65% (wheat) in glumes and 15% (wheat) to 25% (oat) in lemmas of the CO_2 is fixed in C_4 products, while in flag leaves only 2% of the fixed CO_2 can be found in C_4 products. In addition, the rate of CO_2 fixation in the first hour of darkness is 3% and 10% of the CO_2 uptake in the light in glumes and lemmas, respectively, compared with 1% in flag leaves.

In a recent study, Singal et al. (1986) report similar results for wheat ears, without differentiating between the individual bracts. The rate of dark fixation in the ears is 30% of the CO_2 uptake in the light, thus even exceeding the values reported by Wirth et al. (1977). The amount of C_4 fixation is much higher in wheat ears (and typical of C_4 species) than in the C_3–C_4 intermediate species *Moricandia arvensis* (Winter et al. 1982).

Singal et al. (1986) report malate concentrations in wheat ears to decrease after 1 min of incubation, but the decrease is not accompanied by an increase of 3-phosphoglycerate (3-PGA; except in the pericarp of the grains). Hence, in accordance with Wirth et al. (1977), no transfer from malate to Calvin-cycle intermediates could be proved (the PGA pool in fact can change within seconds, so that the determination is very sensitive to time lags during preparation, Stitt 1986). The question of where the CO_2 fixed in C_4 acids is transferred to thus remains unanswered.

The assumption that a C_4 cycle is absent or limited to very low rates in wheat ears is supported by the lack of pyruvate orthophosphate dikinase, an enzyme that is involved in the regeneration of PEP. Meyer et al. (1982) found this enzyme to be present in the aleurone of the green grains of wheat and oat, but not in photosynthesizing tissue of grains, bracts, and leaves, and, moreover, not in the leaves of two C_3–C_4 intermediate plants (*Panicum milioides, Molugo verticilata*).

As a consequence, the regeneration of the CO_2 acceptor, PEP, requires some mechanism other than in C_4 plants, possibly through the respiratory pathway. This regeneration path, however, would compensate for the advantages of dark fixation. Winter et al. (1982) suggest PGA to be a precursor for the synthesis of PEP, which is then used in a secondary carboxylation through PEPCase, and that this malate synthesis is linked to nitrate assimilation.

Wirth et al. (1977) and Singal et al. (1986) agree in the judgement of the ecophysiological significance of their findings: the dark fixation in the pericarp of the CO_2 respired by the grains diminishes the carbon loss. This effect is even enhanced by the dark fixation in the inner bracts, which have stomata facing the grains (Ziegler-Jöns 1989). Moreover, all bracts contain large amounts of heterotrophic tissue releasing CO_2 through respiration.

The gas-exchange data presented here cannot answer the question whether the intermediate values for Γ^* in the ears are caused by a limited rate of C_4 photosynthesis or by some other mechanism. However, the peculiarities of C_3–C_4 intermediate species can explain the characteristic J_m/V_m ratios calculated for the individual bracts, as will be shown.

The sharper separation of the bundle-sheath cells from the intercellular air spaces reduces the conductivity of the cell walls for the uptake of CO_2 and hence also the photosynthesis rates of these cells. This effect is more pronounced at low intercellular partial pressure of CO_2 than at saturating CO_2. To explain the differences in the J_m/V_m ratio, e.g. between inner and outer bracts of oat, this effect would have to reduce the initial slope of the $A(p^c)$ curve of the former by more than 30%. Even under the assumption that no CO_2 uptake occurs in the bundle-sheath cells at low CO_2, their share in the intercellular cell surface has therefore to be more than 30%. This value exceeds by far the values typical for C_4 plants and also those that can be estimated from light-microscopic studies on bracts of ears. Hence, the lower initial slope of the $A(p^c)$ curve in relation to the maximum rate of photosynthesis has to be caused by a second step, the redistribution of RuBPCase from mesophyll cells to bundle-sheath cells. This redistribution results in a lower carboxylation efficiency in mesophyll cells without an equivalent compensation in bundle-sheath cells because of their lower conductivity to CO_2. The distribution of RuBP-

Table 2. Carboxylation efficiency (CE_{M+BS}, $\mu mol \cdot m^{-2} \cdot s^{-1}$ μbar^{-1}) for the individual bracts before anthesis. For treatments *II* of oat and *N* of barley, the values for V_m (μmol $CO_2 \cdot m^{-1} \cdot s^{-1}$) were taken from **Table 1**. For all other treatments, V_m was calculated from the values for J_m (**Table 1**) by division by 2.3. ρ is the ratio of the RuBPCase activities in mesophyll cells to that in bundle-sheath cells. CE_{meas} represents the measured carboxylation efficiencies. Subscripts: M = mesophyll, BS = bundle sheath

Treatment	Oat		Wheat		Barley	
	I	*II*	*I*	*II*	*III*	*N*
J_m	205	264	153	185	179	359
V_m	89	112	67	80	78	165
ρ	0.35	∞	0.35	0.35	0.35	∞
CE_M	0.037	0.134	0.022	0.026	0.026	0.191
CE_{BS}	0.031	0	0.028	0.030	0.030	0
CE_{M+BS}	0.068	0.134	0.050	0.056	0.056	0.191
CE_{meas}	0.076	0.144	0.055	0.062	0.063	0.212

Case is not so important at high CO_2, where mesophyll cells as well as bundle-sheath cells are CO_2-saturated (there might be an influence through higher O_2 partial pressures in the bundle-sheath cells at higher photosynthesis rates, Berry and Farquhar 1978).

In order to evaluate the effect of redistribution of RuBPCase, the initial slopes of the $A(p^c)$ curves were recalculated for all individual bracts of all cultivars examined. The data given by Peisker (1986) for the conductivity of the cell walls of mesophyll cells (2 $\mu mol \cdot m^{-2} \cdot s^{-1}$ μbar^{-1}) and bundle-sheath cells (0.5 $\mu mol \cdot m^{-2} \cdot s^{-1} \cdot \mu bar^{-1}$), and for the ratio of the RuBPCase activity in mesophyll cells to that in bundle-sheath cells, ρ, were taken. For glumes of oat and awns of barley (C_3 types), the values for the carboxylation velocity, V_m, calculated by the usual curve fitting (Table 1) were used. For all other organs, V_m was calculated from the maximum rate of electron transport, J_m, by division by 2.3, the J_m/V_m ratio for glumes of oat and awns of barley. That means that the same J_m/V_m ratio was applied for all treatments.

Appendix B describes the mathematical procedure for the calculation of the initial slopes of the $A(pc)$ curves (or carboxylation efficiencies) for the individual bracts. The numerical data are given in Table 2 and compared with the measured data. The latter are slightly higher than the former for all organs, because the CO_2 gradient between the intercellular air spaces and the chloroplasts has been neglected in the calculation of the maximum carboxylation velocity of RuBPCase (according to Farquhar and von Caemmerer 1982), but not in the recalculation of the initial slope of the $A(p^c)$ curve. However, the agreement between the measured initial slopes of the $A(p^c)$ curves and the calculated values for CE_{M+BS} (carboxylation efficiency of mesophyll and bundle sheath) is striking: under the assumptions (i) that the J_m/V_m ratio is equal for all organs and (ii) that the bracts of wheat ears and the inner bracts of oat and barley ears represent a C_3–C_4 intermediate type, the measured values for the initial slope of the $A(p^c)$ curve can be predicted precisely (this is also true for the values measured two weeks after anthesis, which are not shown here).

By use of the values for the initial slope of the $A(p^c)$ curve given in Table 2, the rate of C_4 fixation can be estimated from the shift of Γ^* (in relation to the values typical for C_3 plants) to be approx. 1 $\mu mol \cdot m^{-2} \cdot s^{-1}$. This is only 1/8 and 1/20 of the activity of PEPCase given by Wirth et al. (1977) and Singal et al. (1986), respectively. If some other mechanism enhancing the refixation of photorespired CO_2 were presupposed (Rawsthorne et al. 1988), the rate of C_4 photosynthesis would even be overestimated from the shift of Γ^*. Values for the coefficient for carbon isotope discrimination ($\delta^{13}C$) for wheat and oat ears (which are similar to those for C_3 plants, Winkler et al. 1978) also give no clue to the presence or absence of a limited rate of C_4 photosynthesis, because the kinetics of the CO_2 uptake in C_3–C_4 intermediate plants are dominated by the kinetics of RuBPCase (Peisker 1986).

Hence, the high activities of PEPcase remain unexplained. They may be advantageous for the dark fixation of respired CO_2, which can then be stored in malate and used in the light. In addition, an ecological advantage under water shortage can be assumed, a situation which is normal for grasses at the time of anthesis and grain filling.

Conclusions

Several characteristics make it reasonable to presuppose a C_3–C_4 intermediate type of photosyn-

thesis in all bracts of wheat ears and in the inner bracts of oat and barley ears of the investigated cultivars:

(i) The activity of enzymes and the fixation of CO_2 in metabolites typical for the C_4 pathway of photosynthesis. These are more significant than in other C_3–C_4 intermediate species.

(ii) The anatomy of these bracts showing bundle-sheath cells with evenly distributed chloroplasts.

(iii) The values for the CO_2-compensation point in the absence of dissimilative respiration, Γ^*, intermediate between the values typical for C_3 and C_4 plants.

(iv) The good agreement of measured initial slopes of the $A(p^c)$ curves with those calculated by use of a model for C_3–C_4 intermediate plants.

From these findings it can be concluded that all bracts of wheat ears as well as inner bracts of oat and barley ears represent C_3–C_4 intermediate organs on a C_3 plant. Glumes of oat and awns of barley, however, represent the normal C_3 type.

The gas-exchange data allow no statement about the presence or absence of a C_4 cycle in ears. If a C_4 cycle is present, it is limited to very low rates compared with the activity of PEPcase. Future experiments should address this question, e.g. by investigation of the O_2 dependence of the CO_2-compensation point and pulse-chase experiments with labelled CO_2.

The mathematical procedures given in *Appendix A* are the result of a cooperation with Dr. H. Selinger, Lehrstuhl für Physik, Freising, FRG. I wish to thank Mrs. U. Mayer, Mr.W. Spitzer, Dr. C. Sautter and Dr. Bartscherer for help with the microscopy and Dr. W.V. Turner for help with the English text. The study was supported by a grant of the Deutsche Forschungsgemeinschaft.

Appendix A: Parameter calculation by fitting model curves to measured photosynthesis rates in response to CO_2 and light

The basic equations are given here without details of the theory (for detailed information on the model see Farquhar and von Caemmerer 1982; Selinger et al. 1987; Ziegler-Jöns and Selinger 1987): eqns. (A1) through (A3) describe the CO_2 response at low CO_2 and saturating light, eqns. (A4) and (A5) the CO_2 response at high CO_2, and eqn. (A6) the light response of the whole-chain electron transport, J. Thus, for any environmental conditions, A is the minimum of the rates calculated from eqns. (A1) and (A4). The CO_2-response curves (see Figs. 1, 2) therefore split into two partial curves described by (A1) and (A4) for low and high CO_2, respectively. The light-response curves is measured at high CO_2 and therefore described by (A4) through (A6).

$$A = V_m \cdot \Pi_1 - D^1 \tag{A1}$$

with the abbreviations

$$\Pi_1 = \frac{p^c - \Gamma^*}{p^c + k'} \tag{A2}$$

$$k' = K^c \cdot (1 + p^0/K^0) \tag{A3}$$

$$A = J \cdot \Pi_2 - D^1 \tag{A4}$$

with the abbreviation

$$\Pi_2 = \frac{p^c - \Gamma^*}{4.5 \cdot p^c + 10.5 \cdot \Gamma^*} \tag{A5}$$

The numbers 4.5 and 10.5 refer to the case where ATP production is the limiting step in RuBP regeneration. When NADPH production is limiting, these numbers have to be replaced by 4 and 8, respectively.

$$\Theta \cdot J^2 - (J_m + q \cdot I) \cdot J + J_m \cdot q \cdot I = 0 \tag{A6}$$

For a given set of n pairs of data $(A_j, \Pi_{1,j})$, $j = 1 \ldots n$, for the CO_2-response curve at low CO_2, the sum of the squares of the deviations from the modelled curve, S_Q, can be calculated as

$$S_Q = \sum (A_j + D^1 - V_m \cdot \Pi_{1,j})^2 \quad j = 1 \ldots n \tag{A7}$$

Exact solutions for the values of V_m and D^1 for which the modelled curve fits the data best can be calculated from the condition that S_Q has to become minimum with respect to changes of V_m and D^1:

$$\frac{\delta S_Q}{\delta D^1} = 0 \tag{A8}$$

$$\frac{\delta S_Q}{\sigma V_m} = 0 \tag{A9}$$

Partial differentiation of (A7) according to (A8) and (A9) yields eqns. (A10) and (A11), respectively.

$$2 \cdot \sum (A_j + D^1 - V_m \cdot \Pi_{1,j}) = 0 \tag{A10}$$

and

$$2 \cdot \sum (A_j + D^1 - V_m \cdot \Pi_{1,j}) \cdot \Pi_{1,j} = 0. \tag{A11}$$

These two equations can be solved for V_m and D^1:

$$V_m = \frac{\sum A_j \cdot \sum \Pi_{1,j} - n \cdot \sum (A_j \cdot \Pi_{1,j})}{(\sum \Pi_{1,j})^2 - n \cdot \sum (\Pi_{1,j})^2} \tag{A12}$$

$$D^1 = (V_m \cdot \sum \Pi_{1,j} - \sum A_j)/n \tag{A13}$$

Thus, the parameters V_m (maximum carboxylation of RuBP-Case) and D^1 (dissimilative respiration in the light) can be calculated from any set of measured data (A_j, p_j^c) of the CO_2 response at low CO_2 and high light by simple summations of the measured values for A, Π_1, $A \cdot \Pi_1^2$. Changes of temperature or the partial pressure of O_2 alter the values for Γ^* and k'.

This procedure is only applicable to parameters which are linear in the basic equations. Above all, it does not work for the light dependence of the rate of whole-chain electron transport, J, eqn. (A6). However, there is a simple way to calculate the parameters q, θ, D^1, and J_m from $A(I)$-data, given access to a personal computer and only a little experience in programming.

For the calculation, reasonable starting values for q, θ, D^1, and J_m have to be chosen (e.g. $q = 0.3$, $\theta = 0.7$, $D^1 = 1\ \mu mol\ m^{-2}\ s^{-1}$, $J_m = 2 \cdot V_m$). For a given set of data (A_j, I_j), values for J_j can be calculated as

$$J_j = (J_m + q \cdot I_j - \sqrt{(J_m + q \cdot I_j)^2 - 4 \cdot \theta \cdot J_m \cdot q \cdot I_j})/(2 \cdot \theta) \tag{A14}$$

and the square deviations of the measured values summed:

$$S_Q = \sum (A_j + D^1 - J_j \cdot \Pi_{2,j})^2 \tag{A15}$$

Thereafter, the programm chooses one of the four parameters at random, changes it at random (in some defined region),

and again calculates the values J_j and the sum S_Q. If S_Q has become smaller, the new parameters are taken as a better fit of the data. After a number of loops, the measured data and the curve are plotted and the procedure stopped or repeated with a new set of starting values.

This method yields numeric values for the absorptance and the efficiency of light use, q, the maximum rate of whole-chain electron transport, J_m, the convexity of the curve, θ, and again for the dissimilative respiration in the light, D^1.

Appendix B: Calculation of the initial slope of the $A(p^c)$ curve for mesophyll cells and bundle-sheath cells

ρ is the ratio of the carboxylation velocity of RuBPCase in mesophyll cells to that in bundle-sheath cells. There is an additional rate of C_4 photosynthesis, which is limited by the rate of PEP regeneration and therefore assumed to be independent of p^c. The equation for the net photosynthesis rate in mesophyll cells, A_M, at low CO_2 given in *Appendix A* (A1 To A3) is modified to

$$A_M=\frac{\rho\cdot V_m}{(1+\rho)}\cdot\frac{p_M^c-\Gamma^*}{p_M^c+k'}-D^1+V_{C4} \tag{B1}$$

The slope of the $A(p^c)$ curve is calculated by differentiation of A_M with respect to p^c, i.e. eqn. (B1) has to be differentiated with respect to p_M^c and multiplied by dp_M^c/dp^c. The partial pressure of CO_2 in the mesophyll cells results from eqn. (B2):

$$p^c-p_M^c=A_M/k_M \tag{B2}$$

and therefore

$$\frac{dp^c}{dp_M^c}=1-\frac{1}{k_M}\cdot\frac{dA_M}{dp^c} \tag{B3}$$

k_M is the conductivity of the mesophyll cell walls for the uptake of CO_2 from the intercellular air spaces. With the assumption that the rate of dissimilative respiration in the light (D^1) as well as the rate of C_4 photosynthesis (V_{C_4}) does not depend on CO_2 partial pressure, the slope of the $A(p^c)$ curve can be written as

$$\frac{dA_M}{dp^c}=\frac{\rho\cdot V_m}{(1+\rho)}\cdot\frac{k'+\Gamma^*}{(p_M^c+k')^2}\cdot\left(1-\frac{1}{k_M}\cdot\frac{dA_M}{dp^c}\right) \tag{B4}$$

The carboxylation efficiency, CE_M, i.e. the initial slope of the $A(p^c)$ curve at $p_M^c=\Gamma^*$, results as

$$CE_M=\frac{\rho\cdot V_m\cdot k_M}{\rho\cdot V_m+k_M\cdot(1+\rho)\,(\Gamma^*+k')} \tag{B5}$$

and in the same way for the bundle-sheath cells

$$CE_{BS}=\frac{V_m\cdot k_{BS}}{V_m+k_{BS}\cdot(1+\rho)\,(\Gamma^*+k')} \tag{B6}$$

The carboxylation efficiency of the whole bract is the sum of both CE_M and CE_{BS},

$$CE_{M+BS}=CE_M+CE_{BS} \tag{B7}$$

because both refer to the projective area and not to the inner surface of the cells.

Additional abbreviations used in appendix A. D^1 = dissimilative respiration in the light ($\mu mol\cdot m^{-2}\cdot s^{-1}$); I = incident PPFD (μmol quanta $\cdot m^{-2}\cdot s^{-1}$); J = rate of whole-chain electron transport ($\mu mol\ e^-\cdot m^{-2}\cdot s^{-1}$); K^c (μbar), K^0 (mbar) = Michaelis-Menten-constants of RuBPCase for CO_2 and O_2, resp.; k' (μbar) = effective Michaelis-Menten-constant; p^0 (mbar) = intercellular partial pressure of O_2; q = parameter for the absorptance and the efficiency of light use (electrons/quanta); S_Q = sum of the squares of the deviations of the measured values from the modelled curve; Π_1, Π_2 = conversion factors (eqns. A2 and A4); θ = convexity factor

Additional abbreviations used in Appendix B. A_M, A_{BS} = net photosynthesis rate in mesophyll cells and bundle-sheath cells, resp.; CE_M, CE_{BS} = carboxylation efficiency (initial slope of the $A(p^c)$ curve) of mesophyll and bundle-sheath cells, resp.; k_M, k_{BS} = conductivity of the mesophyll and the bundle-sheath cell walls, resp., for the uptake of CO_2 from the intercellular airspaces; V_{C_4} = rate of C_4 photosynthesis; ρ = ratio of the RuBPCase activity in the mesophyll cells to that in the bundle-sheath cells

References

Apel, P., Peisker, M. (1979) Pflanzenarten mit intermediärer Merkmalsausprägung in Bezug auf den C_3- und den C_4-pathway der Photosynthese. Kulturpflanze **26**, 99–103

Bauwe, H. (1984) Photosynthetic enzyme activities and immuno-fluorescence studies on the localisation of ribulose-1,5-bisphosphate carboxylase/oxygenase in leaves of C_3, C_4, and C_3–C_4 intermediate species of *Flaveria* (Asteraceae). Biochem. Physiol. Pflanz. **179**, 253–268

Berry, J.A., Farquhar, G.D. (1978) The CO_2 concentrating function of C_4 photosynthesis. A biochemical model. In: Photosynthesis 77, pp. 119–131, Hall, D.O., Coombs, J., Goodwin, T.W., eds. The Biochemical Society, London

Bouton, J.H., Brown, R.H., Evans, P.T., Jernstedt, J.A. (1986) Photosynthesis, leaf anatomy, and morphology of progeny from hybrids between C_3 and C_3–C_4 *Panicum* species. Plant Physiol. **8**, 487–492

Brooks, A., Farquhar, G.D. (1985) Phosphorus nutrition and photosynthesis in spinach leaves: effects on ribulose-1,5-bisphosphate carboxylase activation, quantum yield and contents of some Calvin-cycle metabolites. Aust. J. Plant Physiol. **13**, 221–237

Brown, R.H. (1980) Photosynthesis in grass species differing in carbon dioxide fixation pathways. IV. Analysis of the reduced oxygen response in *Panicum milioides* and *Panicum schenckii*. Plant Physiol. **65**, 346–349

Cock, J.H., Riano, N.M., El-Sharkawy, M.A., López, F.Y., Bastidas, G. (1987) C_3–C_4 intermediate photosynthetic characteristics of cassava (*Manihot esculenta* Crantz). II. Initial products of $^{14}CO_2$ fixation. Photosynthesis Res. **12**, 237–241

Farquhar, G.D., von Caemmerer, S. (1982) Modelling of photosynthetic response to environmental conditions. In: Encyclopedia of plant physiology, N.S., vol. 12B: Physiological plant ecology II, pp. 549–587, Lange, O.L., Nobel, P.S., Osmond, C.B., Ziegler, H., eds. Springer, Berlin Heidelberg New York

Farquhar, G.D., von Caemmerer, S., Berry, J.A. (1980) A biochemical model of photosynthetic CO_2 assimilation in leaves of C_3 species. Planta **149**, 78–90

Gerbaud, A., André, M. (1987) An evaluation of the recycling in measurements of photorespiration. Plant Physiol. **83**, 933–937

Harley, P.C., Tenhunen, J.D., Lange, O.L. (1986) Use of an analytic model to study limitations on net photosynthesis in *Arbutus unedo* under field conditions. Oecologia **70**, 393–401

Holaday, A.S., Lee, K.W., Chollet, R. (1984) C_3–C_4 intermediate species in the genus *Flaveria*: leaf anatomy, ultrastruc-

ture, and the effect of O_2 on the CO_2 compensation concentration. Planta **160**, 25–32

Holaday, A.S., Shieh, Y.-J., Lee, K.W., Chollet R. (1981) Anatomical, ultrastructural and enzymic studies of leaves of *Moricandia arvensis*, a C_3–C_4 intermediate species. Biochem. Biophys. Acta **637**, 334–341

Hunt, S., Smith, A.M., Woolhouse, H.W. (1987) Evidence for a light-dependent system for reassimilation of photorespiratory CO_2, which does not include a C_4 cycle, in the C_3–C_4 intermediate species *Moricandia arvensis*. Planta **171**, 227–234

Jenner, C.F., Rathjen, A.J. (1972) Factors limiting the supply of sucrose to the developing wheat grain. Ann. Bot. **36**, 729–741

Knoppik, D., Selinger, H., Ziegler-Jöns, A. (1986) Differences between the flag leaf and the ear of a spring wheat cultivar (*Trit. aestivum* cv. Arkas) with respect to the CO_2 response of assimilation, respiration, and stomatal conductance. Physiol. Plant. **68**, 451–457

Laisk, A. (1983) Calculation of leaf photosynthetic parameters considering the statistical distribution of stomatal apertures. J. Exp. Bot. **34**, 1627–1635

Meidner, H. (1986) Cuticular conductance and the humidity response of stomata. J. Exp. Bot. **37**, 517–525

Meyer, A.O., Kelly, G.J., Latzko, E. (1982) Pyruvate orthophosphate dikinase from the immature grains of cereal grasses. Plant Physiol. **69**, 7–10

Peisker, M. (1986) Models of carbon metabolism in C_3–C_4-intermediate plants as applied to the evolution of C_4-photosynthesis. Plant Cell Environ. **9**, 627–635

Peisker, M., Bauwe, H. (1984) Modelling carbon metabolism in C_3–C_4 intermediate species. 1. CO_2 compensation concentration and its O_2 dependence. Photosynthetica **18**, 9–19

Perrot-Rechenmann, C., Chollet, R., Gadal, P. (1984) In-situ immunofluorescent localization of phosphoenolpyruvate and ribulose 1,5-bisphosphate carboxylases in leaves of C_3, C_4, and C_3–C_4 intermediate *Panicum* species. Planta **161**, 266–271

Radley, M. (1981) The effect on wheat grain growth of the removal or ABA treatment of glumes and lemmas. J. Exp. Bot. **32**, 129–140

Rathnam, C.K.M., Chollet, R. (1979) Photosynthetic carbon metabolism in *Panicum milioides*, a C_3–C_4 intermediate species: evidence for a limited C_4 dicarboxylic acid pathway of photosynthesis. Biochim. Biophys. Acta **548**, 500–519

Rawsthorne, S., Hylton, C.M., Smith, A.M., Woolhouse, H.W. (1988) Photorespiratory metabolism and immunogold localization of photorespiratory enzymes in leaves of C_3 and C_3–C_4 intermediate species of *Moricandia*. Planta **173**, 298–308

Schönherr, J. (1982) Resistance of plant surfaces to water loss. Transport properties of cutin, suberin, and associated lipids. In: Encyclopedia of plant physiology, N.S., vol. 12B: Physiological plant ecology II, pp. 153–179, Lange, O.L., Nobel, P.S., Osmond, C.B., Ziegler, H., eds. Springer, Berlin Heidelberg New York

Selinger, H., Knoppik, D., Ziegler-Jöns, A. (1987) Gas exchange of flag leaves and ears of wheat. Interpretation on the basis of a photosynthesis model. In: Progress in photosynthesis research, vol. IV, pp. 229–232, Biggins, J., ed. Martinus Nijhoff Publishers, Dordrecht

Singal, H.R., Sheoran, I.S., Randhir Singh (1986) In vitro enzyme activities and products of $^{14}CO_2$ assimilation in flag leaf and ear parts of wheat (*Triticum aestivum* L.). Photosynthesis Res. **8**, 113–122

Stitt, M. (1986) Limitation of photosynthesis by carbon metabolism. I. Evidence for excess electron transport capacity in leaves carrying out photosynthesis in saturating light and CO_2. Plant Physiol. **81**, 1115–1122

von Caemmerer, S., Farquhar, G.D. (1981) Some relationships between the biochemistry of photosynthesis and the gas exchange of leaves. Planta **153**, 273–278

Winkler, F.J., Wirth, E., Latzko, E., Schmidt, H.-L., Hoppe, W., Wimmer, P. (1978) Einfluß von Wachstumsbedingungen und Entwicklung auf $\delta^{13}C$-Werte in verschiedenen Organen und Inhaltsstoffen von Weizen, Hafer und Mais. Z. Pflanzenphysiol. **87**, 255–263

Winter, K., Usuda, H., Tsuzuki, M., Schmitt, M., Edwards, G.E., Thomas, R.J., Evert, R.F. (1982) Influence of nitrate and ammonia on photosynthetic characteristics and leaf anatomy of *Moricandia arvensis*. Plant Physiol. **70**, 616–625

Wirth, E., Kelly, G.J., Fischbeck, G., Latzko, E. (1977) Enzyme activities and products of CO_2 fixation in various photosynthetic organs of wheat and oat. Z. Pflanzenphysiol. **82**, 78–87

Wong, S.C., Cowan, I.R., Farquhar, G.D. (1985a) Leaf conductance in relation to rate of CO_2 assimilation. I. Influence of nitrogen nutrition, phosphorus nutrition, photon flux density, and ambient partial pressure of CO_2 during ontogeny. Plant Physiol. **78**, 821–825

Wong, S.C., Cowan, I.R., Farquhar, G.D. (1985b) Leaf conductance in relation to rate of CO_2 assimilation. II. Effects of short-term exposures to different photon flux density. Plant Physiol. **78**, 826–829

Wong, S.C., Cowan, I.R., Farquhar, G.D. (1985c) Leaf conductance in relation to rate of CO_2 assimilation. III. Influence of water stress and photoinhibition. Plant Physiol. **78**, 830–834

Ziegler-Jöns, A. (1989) Gas exchange of ears of cereals in response to CO_2 and light. 1. Relative contributions of parts of ears of wheat, oat, and barley to the gas exchange of the whole organ. Planta 178:84–91

Ziegler-Jöns, A., Selinger, H. (1987) Calculation of leaf photosynthetic parameters from light-response curves for ecophysiological applications. Planta **171**, 412–415

Ziegler-Jöns, A., Knoppik, D., Selinger, H. (1986) The calibration of thermocouples for leaf temperature measurements in gas exchange cuvettes. Oecologia **68**, 611–614

Ziegler-Jöns, A., Knoppik, D., Selinger, H. (1987) Characteristics of the CO_2 exchange of wheat ears. In: Progress in photosynthesis research, vol. IV, pp. 233–236, Biggins, J., ed. Martinus Nijhoff Publishers, Dordrecht

Received 8 August; accepted 6 December 1988